nature materials

LETTERS

PUBLISHED ONLINE: 24 MAY 2009 | DOI: 10.1038/NMAT2466

Local ordering and electronic signatures of submonolayer water on anatase TiO_2(101)

Yunbin He[1]*, Antonio Tilocca[2], Olga Dulub[1], Annabella Selloni[3] and Ulrike Diebold[1]†

The interaction of water with metal oxide surfaces is of fundamental importance to various fields of science, ranging from geophysics to catalysis and biochemistry[1–4]. In particular, the discovery that TiO_2 photocatalyses the dissociation of water[5] has triggered broad interest and intensive studies of water adsorption on TiO_2 over decades[6]. So far, these studies have mostly focused on the (110) surface of the most stable polymorph of TiO_2, rutile, whereas it is the metastable anatase form that is generally considered photocatalytically more efficient. The present combined experimental (scanning tunnelling microscopy) and theoretical (density functional theory and first-principles molecular dynamics) study gives atomic-scale insights into the adsorption of water on anatase (101), the most frequently exposed surface of this TiO_2 polymorph. Water adsorbs as an intact monomer with a computed binding energy of 730 meV. The charge rearrangement at the molecule–anatase interface affects the adsorption of further water molecules, resulting in short-range repulsive and attractive interactions along the [010] and [11$\bar{1}$]/[1$\bar{1}\bar{1}$] directions, respectively, and a locally ordered (2 × 2) superstructure of molecular water.

As TiO_2 is a technologically important material, much effort has been devoted to understand how water adsorbs at its surfaces. Surface-science studies on well-characterized surfaces have yielded much detail of the water/TiO_2 system[1,6,7]. In particular, extensive scanning tunnelling microscopy (STM) work has focused on investigating the role of surface oxygen vacancies that are prominent on the (110) surface of the most stable TiO_2 polymorph, rutile, on which almost all studies so far have been carried out[7–10]. However, technical TiO_2 is very often of the (metastable) anatase form; most TiO_2 nanomaterials are of anatase form, and in many cases anatase is photocatalytically more active than rutile. This has motivated theoretical investigations of anatase[11–13], but there are hardly any experiments on well-characterized surfaces that would enable verification of these theoretical predictions. This lack of experimental data is mostly due to the limited availability of anatase crystals of sufficiently large size[14].

We circumvent this problem by using appropriate mineral samples. The structure of anatase (101), the surface with the lowest energy, is now well understood[15]: it has a saw-tooth-like morphology with five-fold coordinated Ti (Ti_{5c}) and two-fold coordinated surface O (O_{2c}) atoms arranged in rows along the [010] direction (Fig. 1a). The only previous experimental study of water on anatase (101) (ref. 16), a combined temperature-programmed desorption and X-ray photoelectron spectroscopy investigation, has revealed that water adsorbs molecularly, in accordance with density functional theory (DFT) calculations[11,12]. These DFT studies predict that the water molecule is bound to a Ti_{5c} atom and forms weak hydrogen bonds with the two neighbouring O_{2c} atoms. Here,

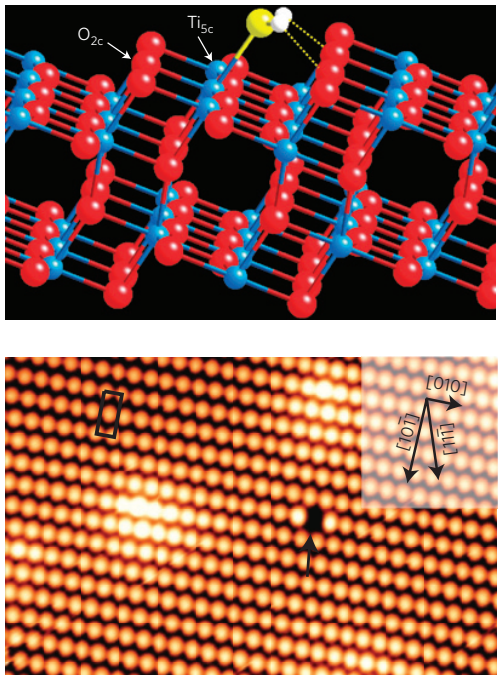

Figure 1 | The TiO_2 anatase (101) surface. a, Ball-and-stick model with an adsorbed water molecule. Water oxygen and hydrogen atoms are plotted in yellow and white, respectively, whereas TiO_2 atoms are blue (Ti) and red (O). **b**, Empty-states STM image of the clean surface (115 × 72 Å^2, $V_{sample} = +1.61$ V, $I_{Tunnel} = 1.58$ nA), taken at room temperature. Each oval-shaped bright spot extends across both undercoordinated surface O_{2c} and Ti_{5c} atoms. The centred rectangular surface unit cell, marked in **b**, contains two equivalent Ti_{5c}/O_{2c} surface atoms. The arrow marks a water monomer, probably adsorbed at a subsurface defect site.

we report that the electronic changes that are imparted by such an adsorbed water monomer to the anatase (101) surface lead to repulsive/attractive intermolecular interactions along/across rows. The resulting changes in the binding energy and the dynamical behaviour of adsorbed water explain the experimentally observed tendency for the ordering of molecules on anatase (101).

An STM image of the clean anatase (101) surface, taken at room temperature, is shown in Fig. 1b. Each atomic-sized, oval spot extends across an O_{2c} and Ti_{5c} (ref. 15). The large, bright spots that reach across over many lattice sites are attributed to subsurface impurities in the mineral sample[17]. Different from rutile (110), the

[1]Department of Physics, Tulane University, New Orleans, Louisiana 70118, USA, [2]Department of Chemistry and Materials Simulation Laboratory, University College London, London WC1H 0AJ, UK, [3]Department of Chemistry, Princeton University, Princeton, New Jersey 08544, USA. *Present address: Faculty of Materials Sciences and Engineering, Hubei University, No. 11 Xueyuan Road, Wuchang, Wuhan 430062, China. †e-mail: diebold@tulane.edu.

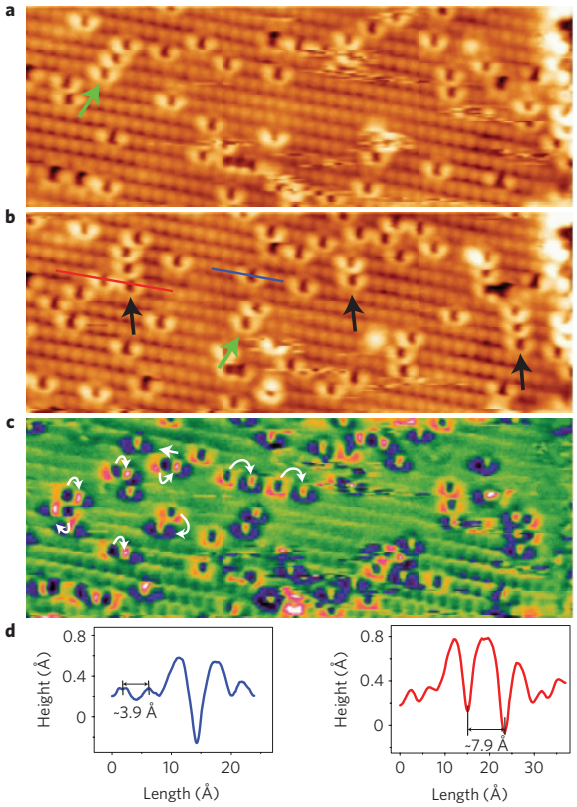

Figure 2 | Hopping and short-range ordering of water on anatase (101). **a**,**b**, Two consecutive STM images of 0.11 ML of water on anatase (101) (173×63 Å^2, +3.5 V, 0.45 nA) taken at a sample temperature of 190 K. The green and black arrows indicate ordered water clusters along the [11$\bar{1}$] and [11$\bar{1}$] directions, respectively. **c**, Difference image (**a**,**b**); the white arrows indicate the hopping direction of selected water molecules. **d**, Line profiles of a water molecule, taken across the blue line in **b**, and of two adsorbed water molecules separated by an empty lattice site (red line in **b**).

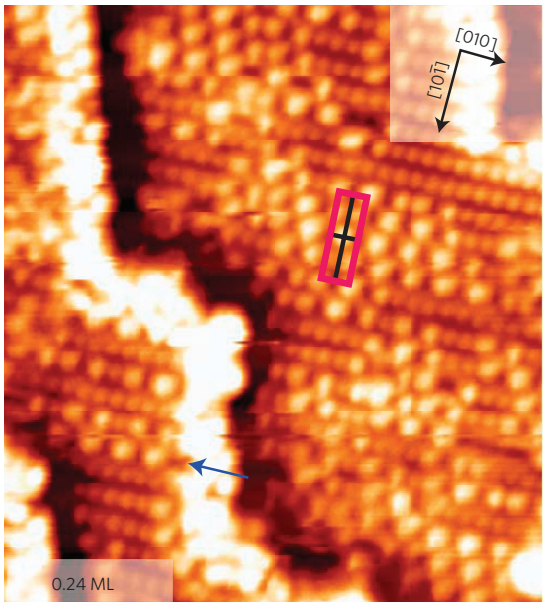

Figure 3 | Ordered water overlayer on anatase (101). STM image (118×127 Å^2, +1.49 V, 0.28 nA) of the anatase TiO_2(101) surface after water adsorption at 150 K. The water coverage is 0.24 ML. The water forms a weakly ordered overlayer with (2×2) symmetry as indicated by the unit cell. The blue arrow indicates the double periodicity along the [010] direction.

clean anatase (101) surface shows very few atomic-size defects. In particular there are hardly any O vacancies, which are known to have an important role in the surface chemistry of rutile (110) (refs 6, 7). In fact, our DFT calculations predict that O vacancies on anatase TiO_2 (101) have a substantially lower formation energy at subsurface than at surface sites, and STM results from a reduced anatase sample show that intrinsic defects reside predominantly in the subsurface region[17]. The STM image in Fig. 1b also shows an isolated black spot, with a brighter spot on either side (marked by an arrow). As we will argue below, such a white–black–white (w–b–w) feature is attributed to an adsorbed water monomer. At room temperature, the number of these w–b–w features is small, and their density is higher for more reduced samples. For the crystal used here, the saturation coverage is about 0.005 monolayers (where one monolayer (ML) corresponds to the number of Ti_{5c} sites per unit area). Water desorbs slightly below room temperature from the defect-free surface[16], but the above-mentioned subsurface defects increase the adsorption energy of water molecules. Thus, the water molecule in Fig. 1b probably sits on a site with a subsurface defect.

When the clean anatase (101) surface is exposed to water at low temperatures, the number of w–b–w features increases (Fig. 2). As shown in the line profile across one such feature, the apparent depression is ~1 Å deep. The apparent elevation at each neighbouring lattice site extends towards the adjacent row in the [10$\bar{1}$] direction. Figure 2 shows two consecutive STM images with a surface coverage of 0.11 ML. At the sample temperature where the images were taken (190 K), the w–b–w features show some mobility. They always hop as a whole unit. This appears more clearly in the difference image in Fig. 2c. (The two images in Fig. 2a,b are part of a longer series, which follows the motion of the w–b–w features, see Supplementary Movie S1.)

A short-range ordering is also apparent in Fig. 2: the w–b–w features tend to align along the [11$\bar{1}$] and [1$\bar{1}\bar{1}$] directions, that is, along the diagonal of the centred unit cell (see also Supplementary Fig. S1). Interestingly, we rarely observe two neighbouring black spots sitting right next to each other on one row, and the red line profile in Fig. 2d shows that the black spots are separated by two lattice spacings along [010]. This is also true for higher water coverages (Fig. 3), where, instead of longer, black rows, STM shows lines with alternating w–b contrast on neighbouring sites. This double periodicity along the rows, combined with the tendency to have a w–b–w neighbour in the next row, results in the formation of a superstructure with (2×2) symmetry. The STM image in Fig. 3 shows patches of this superstructure.

These experimental results are consistent with each w–b–w unit representing a water monomer (see also Supplementary Fig. S2), but alternative possibilities need to be considered. Water–water interactions are usually attractive, yet the double periodicity along the [010] direction would point towards a repulsive interaction between water monomers. Is it possible that, instead of an isolated monomer, each w–b–w unit represents a particularly stable water aggregate, containing two, three or even more molecules[13,18,19]? Such a cluster should contain a water molecule in a special configuration that gives rise to the prominent black spot in empty-states STM. In addition, the water clusters should not break up when hopping across the surface, and they should somehow preserve their special configuration when aligning themselves into rows. On reduced surfaces with subsurface defects, we observe w–b–w features even at 400 K. The typical strength of a H-bond is ~0.2 eV. Thus, it is quite unlikely that a H-bonded water cluster

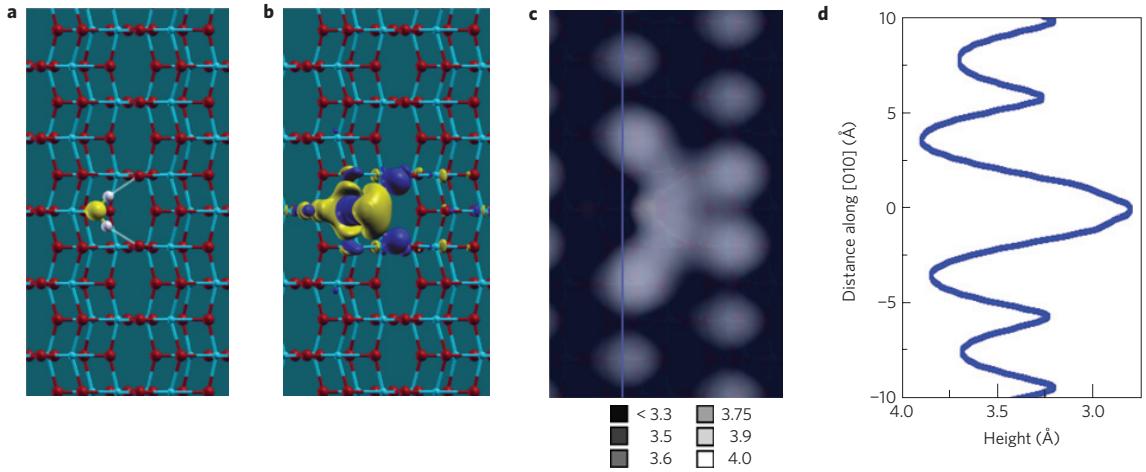

Figure 4 | Theoretical results for an adsorbed water monomer on anatase (101). a,**b**, Optimized geometry (top view) (**a**) and isosurface (**b**) of the charge density difference resulting from adsorption of a water molecule. Positive (electron excess) and negative (electron deficit) lobes are shown in blue and yellow, respectively. **c**, Simulated constant density (1×10^{-4} electrons per bohr^3) image, determined from the integrated local density of states in an energy window of 2.75 eV from the conduction band minimum. **d**, Height profile along the line indicated in **c**; *z* values in the plot and the height profile are referenced to the position of the Ti_{5c} atoms.

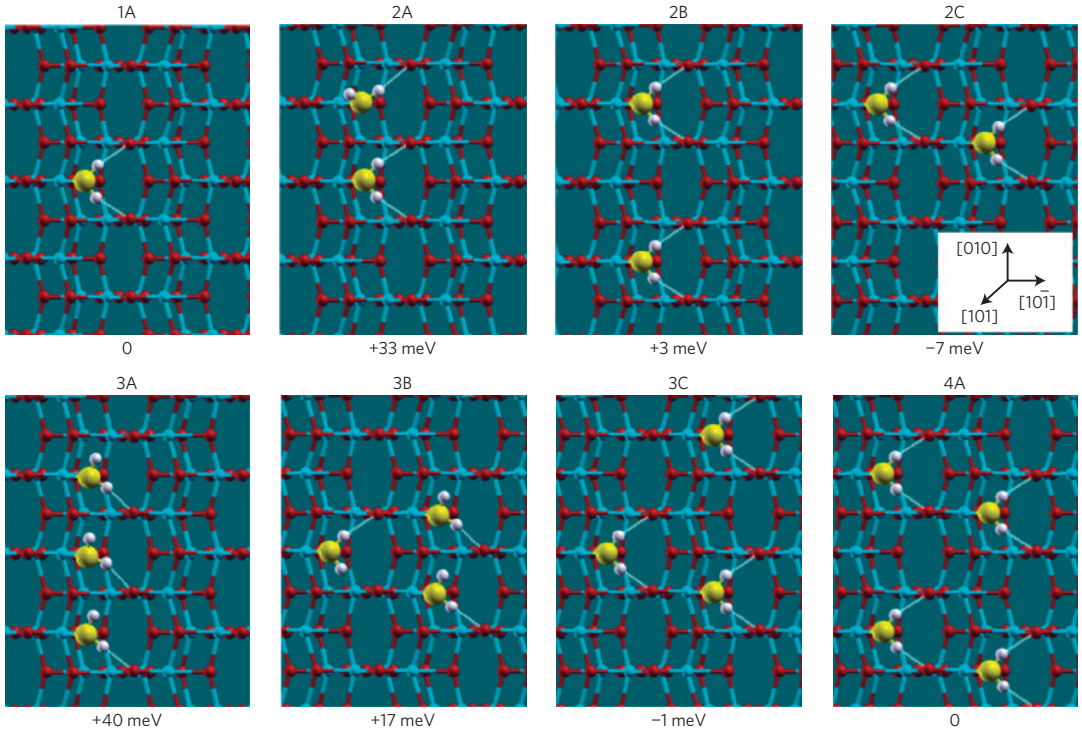

Figure 5 | Calculated adsorption configurations of water on anatase (101). Optimized structures of a water monomer (1A), and of different clusters of two (2A, 2B and 2C), three (3A, 3B and 3C) and four (4A) water molecules. The adsorption energy for each configuration is given in millielectronvolts per water molecule, relative to the adsorbed monomer; a positive value indicates that the configuration is less stable relative to isolated monomers.

could be stable at and even above room temperature; nevertheless, this possibility was explored using Car–Parrinello[20] first-principles molecular dynamics (FPMD) simulations.

The computed adsorption structure of an isolated H_2O molecule is shown in Fig. 4a: the water oxygen forms a dative bond with a surface Ti_{5c}, whereas the hydrogens form two weak H-bonds with bridging oxygens ($R_{O\text{–}O} = 3.15$ Å; $R_{H\text{–}O} = 2.30$ Å). Its adsorption energy is computed as −730 meV, where the negative energy means the adsorption is exothermic. In the simulated STM images (Fig. 4c and Supplementary Fig. S3), a bright feature is observed at the position of the water molecule, displaced towards [10$\bar{1}$] with respect to the Ti_{5c} adsorption site. The Ti_{5c} adsorption site appears as a dark spot, whereas the two neighbouring Ti_{5c} sites in the same row and especially the two Ti_{5c} sites in the adjacent row on the right give rise to further bright features. Only the monomer shows an apparent depression at a Ti_{5c} site that is deeper than a regular lattice

site. Water dimers have a very different appearance; for example, the structure recently proposed by Mattioli *et al.*[13] shows a weak feature extending two lattice sites along a single row. Similarly, all of the statistically relevant configurations of a water trimer give STM contrasts that do not resemble the experimental STM images (see Supplementary Fig. S4). In the calculated as well as the experimental images, each water molecule affects a relatively large area, suggesting that the adsorbed water molecule modifies the electron charge distribution at surrounding Ti_{5c} sites. Figure 4b shows the electronic charge density difference induced by an adsorbed water molecule. The yellow lobes enclose regions where the density is reduced on adsorption. Such a reduction is clearly present on both of the two Ti_{5c} atoms in the adjacent row. It is attributed to the H-bonds between the water molecule and the two O_{2c} atoms bonded to the Ti_{5c} adsorption sites in the adjacent row.

FPMD simulations of an isolated adsorbed water molecule (see Supplementary Fig. S5) show that the molecular orientation is largely maintained along the trajectory, with the dipole always pointing roughly towards [10$\bar{1}$]. In contrast, when a second H_2O is adsorbed on an adjacent Ti_{5c} site along the same row, the FPMD traces (see Supplementary Fig. S5, centre) show a marked in-plane and out-of-plane motion of the two molecules, suggesting intermolecular interactions. This is confirmed by the optimized structure (2A in Fig. 5), in which one of the two molecules is turned sideways, with a hydrogen pointing upward. Correspondingly, the adsorption energy per molecule (also reported in Fig. 5) is slightly reduced from that of an isolated monomer, indicating a small but significant repulsion between the two adjacent molecules. This repulsive interaction is largely removed when the two molecules are adsorbed at next-nearest-neighbouring Ti_{5c} sites along the same row, see structure 2B in Fig. 5, in agreement with the experimentally observed double periodicity. In contrast, the adsorption of two molecules at neighbouring Ti_{5c} sites in adjacent rows (structure 2C in Fig. 5) is slightly favoured, probably because the reduced charge density at these Ti_{5c} sites renders them slightly more acidic. A similar effect was observed in other adsorbate/oxide systems[21].

Our calculations for three and four adsorbed water molecules (Fig. 5 bottom row, and Supplementary Fig. S5) confirm the occurrence of (weak) attractive interactions between neighbouring water molecules along [11$\bar{1}$]/[1$\bar{1}\bar{1}$], and repulsive interactions between molecules at neighbouring Ti_{5c} sites along [010]. Consider, for example, the adsorption energies of three water molecules: adsorption is least favoured when all molecules are adsorbed in a single row (structure 3A), it becomes slightly stronger when one molecule is moved to an adjacent row (3B) and further increases when another molecule is moved one lattice spacing away (3C). Although the computed energy differences for the various investigated configurations are small, they are in excellent agreement with the short-range ordering observed in STM.

This interplay between substrate-mediated intermolecular attractive and repulsive interactions that determines ordering at low water coverage is a novel effect. On metal surfaces the hydrogen bonding between water molecules results in clusters in various configurations[18,19,22]. It is well established[1,4] that the surface oxygen atoms (O_s) on metal oxides influence the adsorption properties by providing extra possibilities for H-bonding. The formation of ordered overlayers has been observed on some oxide surfaces[23,24], but usually it is either the registry with the substrate, or the H-bonding between water molecules, that dictates the formation of such ordering, rather than substrate-mediated interactions. The effect reported here originates from the stronger water–surface (730 meV) versus water–water interaction (for which an upper limit is the cohesive energy of ice, ~580 meV), and the possibility for each water molecule to form two H-bonds with the anatase (101) surface. These features are not present on the other TiO_2 polymorph, rutile (110), where STM shows water molecules adsorbed right next to each other along Ti_{5c} rows[10], and DFT calculations indicate intermolecular H-bonding and potentially dissociation even on the stoichiometric surface[8,25,26]. More generally, the situation described in this work—namely, that an O_s atom can accommodate only one H-bond from an adsorbed water molecule, and that, after arrival of a second water molecule in its neighbourhood, the competition between the two molecules for the same O_s atom weakens the H-bond of the first one and effectively lowers its adsorption energy—could be a general feature that has to be taken into account when considering water on oxides.

Methods

Experimental details. All experiments were carried out in an ultrahigh-vacuum chamber with a base pressure of $\sim 1 \times 10^{-10}$ mbar (SPECS GmbH). It is equipped with a variable-temperature Aarhus STM, and facilities for low-energy electron diffraction, X-ray photoelectron spectroscopy, surface cleaning and gas dosing. *In situ* sample cleaning was achieved by cycles of Ar^+ ion sputtering and annealing to 600 °C. The anatase sample was a natural mineral crystal, cleaved *ex situ*. Water was cleaned by repeated freeze–pump–thaw cycles and the purity of water vapour was checked by mass spectrometry. It was dosed by backfilling the chamber through a leak valve with the sample in the cold stage of the STM. The tip was retracted by ~1 mm from the sample to avoid tip shadowing effects. Typically, water was dosed at a sample temperature between 100 and 130 K with nominal dosages of less than one Langmuir (L, where 1 L equals a dose of 1×10^{-6} torr s). STM was carried out in the constant-current mode, and empty states were typically imaged with positive sample bias voltages in the range of 0.6–3.5 V and tunnelling currents between 0.2 and 1.1 nA.

Theoretical details. For the DFT calculations, we used the Perdew–Burke–Ernzerhof exchange–correlation functional[27] and ultrasoft pseudopotentials[28]. Valence electrons included the O 2*s*, 2*p* and Ti 3*s*, 3*p*, 3*d*, 4*s* shells; the energy cutoffs for the smooth part of the wavefunctions and the augmented density were 25 and 200 Ryd, respectively; k-sampling was restricted to only the Γ point. The stoichiometric anatase (101) surface was modelled as a periodically repeated slab including four Ti_8O_{16} layers, with a vertical separation between slabs of ~12 Å. A (1×4) supercell with an exposed surface area of 10.24×15.14 Å^2 was used. Such a large surface cell enables us to reduce the interaction between periodic images of the adsorbed molecules, effectively modelling isolated molecules. In all simulations, the atoms of the bottom layer were fixed to their equilibrium bulk positions, and water was adsorbed only on the upper surface. The average adsorption energy per water molecule is defined as $E_{ads} = [E(\text{slab} + nH_2O) - E(\text{slab}) - nE(H_2O)]/n$, where $E(\text{slab} + nH_2O)$ and $E(\text{slab})$ are the energy of the slab with and without water molecules, respectively, $E(H_2O)$ is the energy of a gas-phase water molecule and n is the number of water molecules adsorbed. FPMD trajectories of 10–15 ps at 160 K were carried out to probe the configurational space of the adsorbed molecules; selected configurations extracted from these trajectories were optimized using the PWSCF code of the Quantum-Espresso package[29], until the largest component in the ionic forces was less than 25 meV Å^{-1}. These optimized structures were then used as input for the calculations of empty-state STM images[30].

Received 22 December 2008; accepted 30 April 2009; published online 24 May 2009

References

1. Henderson, M. A. The interaction of water with solid surfaces: Fundamental aspects revisited. *Surf. Sci. Rep.* **46**, 1–308 (2002).
2. Verdaguer, A., Sacha, G. M., Bluhm, H. & Salmeron, M. Molecular structure of water at interfaces: Wetting at the nanometer scale. *Chem. Rev.* **106**, 1478–1510 (2006).
3. Al-Abadleh, H. A. & Grassian, V. H. Oxide surfaces as environmental interfaces. *Surf. Sci. Rep.* **52**, 63–161 (2003).
4. Thiel, P. A. & Madey, T. E. The interaction of water with solid surfaces: Fundamental aspects. *Surf. Sci. Rep.* **7**, 211–385 (1987).
5. Fujishima, A. & Honda, K. Electrochemical photolysis of water at a semiconductor electrode. *Nature* **238**, 37–38 (1972).
6. Diebold, U. The surface science of titanium dioxide. *Surf. Sci. Rep.* **48**, 53–229 (2003).
7. Pang, C. L., Lindsay, R. & Thornton, G. Chemical reactions on rutile TiO_2(110). *Chem. Soc. Rev.* **37**, 2328–2353 (2008).
8. Wendt, S. *et al.* Formation and splitting of paired hydroxyl groups on reduced TiO_2(110). *Phys. Rev. Lett.* **96**, 066107 (2006).
9. Zhang, Z., Bondarchuk, O., Kay, B. D., White, J. M. & Dohnalek, Z. Imaging water dissociation on TiO_2(110): Evidence for inequivalent geminate OH groups. *J. Phys. Chem. B* **110**, 21840–21845 (2006).
10. Brookes, I. M., Muryn, C. A. & Thornton, G. Imaging water dissociation on TiO_2(110). *Phys. Rev. Lett.* **87**, 266103 (2001).

11. Vittadini, A., Selloni, A., Rotzinger, F. P. & Graetzel, M. Structure and energetics of water adsorbed at TiO_2 anatase (101) and (001) surfaces. *Phys. Rev. Lett.* **81**, 2954–2957 (1998).
12. Tilocca, A. & Selloni, A. Vertical and lateral order in adsorbed water layers on anatase TiO_2(101). *Langmuir* **20**, 8379–8384 (2004).
13. Mattioli, G., Filippone, F., Caminiti, R. & Bonapasta, A. A. Short hydrogen bonds at the water/TiO_2 (anatase) interface. *J. Phys. Chem. C* **112**, 13579–13586 (2008).
14. Diebold, U., Ruzycki, N., Herman, G. S. & Selloni, A. One step towards bridging the materials gap: Surface studies of TiO_2 anatase. *Catal. Today* **85**, 93–100 (2003).
15. Gong, X. -Q., Selloni, A., Batzill, M. & Diebold, U. Steps on anatase TiO_2(101). *Nature Mater.* **5**, 665–670 (2006).
16. Herman, G. S., Dohnalek, Z., Ruzycki, N. & Diebold, U. Experimental investigation of the interaction of water and methanol with anatase-TiO_2(101). *J. Phys. Chem. B* **107**, 2788–2795 (2003).
17. He, Y. B., Dulub, O., Cheng, H. Z., Selloni, A. & Diebold, U. Evidence for the predominance of subsurface defects on reduced anatase TiO_2(101). *Phys. Rev. Lett.* **102**, 106105 (2009).
18. Cerda, J. *et al.* Novel water overlayer growth on Pd(111) characterized with scanning tunneling microscopy and density functional theory. *Phys. Rev. Lett.* **93**, 116101 (2004).
19. Michaelides, A. & Morgenstern, K. Ice nanoclusters at hydrophobic metal surfaces. *Nature Mater.* **6**, 597–601 (2007).
20. Car, R. & Parrinello, M. Unified approach for molecular dynamics and density-functional theory. *Phys. Rev. Lett.* **55**, 2471–2474 (1985).
21. Wang, Y. *et al.* Tuning the reactivity of oxide surfaces by charge-accepting adsorbates. *Angew. Chem. Int. Ed.* **46**, 7315–7318 (2007).
22. Mitsui, T., Rose, M. K., Fomin, E., Ogletree, D. F. & Salmeron, M. Water diffusion and clustering on Pd(111). *Science* **297**, 1850–1852 (2002).
23. Ferry, D. *et al.* The properties of a two-dimensional water layer on MgO(001). *Surf. Sci.* **377–379**, 634–638 (1997).
24. Dulub, O., Meyer, B. & Diebold, U. Observation of the dynamical change in a water monolayer adsorbed on a ZnO surface. *Phys. Rev. Lett.* **95**, 136101 (2005).
25. Lindan, P. J. D. & Zhang, C. Exothermic water dissociation on the rutile TiO_2(110) surface. *Phys. Rev. B* **72**, 075439 (2005).
26. Kowalski, P. M., Meyer, B. & Marx, D. Composition, structure, and stability of the rutile TiO_2(110) surface: Oxygen depletion, hydroxylation, hydrogen migration, and water adsorption. *Phys. Rev. B* **79**, 115410 (2009).
27. Perdew, J. P., Burke, K. & Ernzerhof, M. Generalized gradient approximation made simple. *Phys. Rev. Lett.* **77**, 3865–3868 (1996).
28. Vanderbilt, D. Soft self-consistent pseudopotentials in a generalized eigenvalue formalism. *Phys. Rev. B* **41**, 7892–7895 (1990).
29. Baroni, S., Giannozzi, P., De Gironcoli, S. & Dal Corso, A. *Quantum ESPRESSO v. 3.2.3*, <http://www.pwscf.org>.
30. Tersoff, J. & Hamann, D. R. Theory of the scanning tunneling microscope. *Phys. Rev. B* **31**, 805–813 (1985).

Acknowledgements

This work was supported by DoE award DE-FG02-05ER15702. We thank C. Di Valentin for participating in the early stages of this project and H. Cheng for the constant density STM program. A.T. thanks the UK's Royal Society for financial support.

Additional information

Supplementary information accompanies this paper on www.nature.com/naturematerials. Reprints and permissions information is available online at http://npg.nature.com/reprintsandpermissions. Correspondence and requests for materials should be addressed to U.D.